SRF 020220-02

CORRECTION OF THE COUPLING OF CESR RF CAVITIES TO KLYSTRONS USING THREE-POST WAVEGUIDE TRANSFORMERS

V. Veshcherevich and S. Belomestnykh

INTRODUCTION

Superconducting CESR RF cavities were designed to handle high RF power delivered to the beam from klystron amplifiers (operating frequency 499.765 MHz). They are strongly overcoupled so that having high Q of the order of 10^9 they have couplers with external Q_{ext} of only 2×10^5. At a low beam current in the machine, almost full power is reflected from the cavity and goes to the load due to a ferrite circulator mounted between RF cavity and the klystron. With the beam current increasing, the power delivered to the beam goes up and the reflected power goes down. At a certain beam current the reflected power vanishes and the cavity turns perfectly matched to the waveguide power transmission line. If the beam current continues to rise the power reflection reappears and both delivered and reflected powers increase with the beam current.

For power efficiency, the matched condition should be reached at the highest beam current in the machine. At CESR, however, due to machine parameters upgrade during last years the matching occurs at a beam current of around $^2/_3$ of the highest value (see Figure 1). In consequence of this, there is a lower efficiency of the RF system and excessive a. c. power consumption at highest beam currents.

It is reasonable to decrease the Q_{ext} of RF cavities for lowering reflection at high CESR beam current. The cavity coupler design makes it impossible to vary the coupling and hence the Q_{ext}. However, it is possible to do this with impedance transformers outside the cavities. To this end waveguide three-post impedance transformers were designed, made, and mounted into the waveguides between each cavity and the klystrons.

Using impedance transformers, it is possible to go up in Q_{ext} as well as down. This will be useful in the future for CESR-c project when beam loading will be significantly low. The transformers can be used also for adjusting cavity loads connected to the same klystron via a magic tee for obtaining better power and cavity field balance.

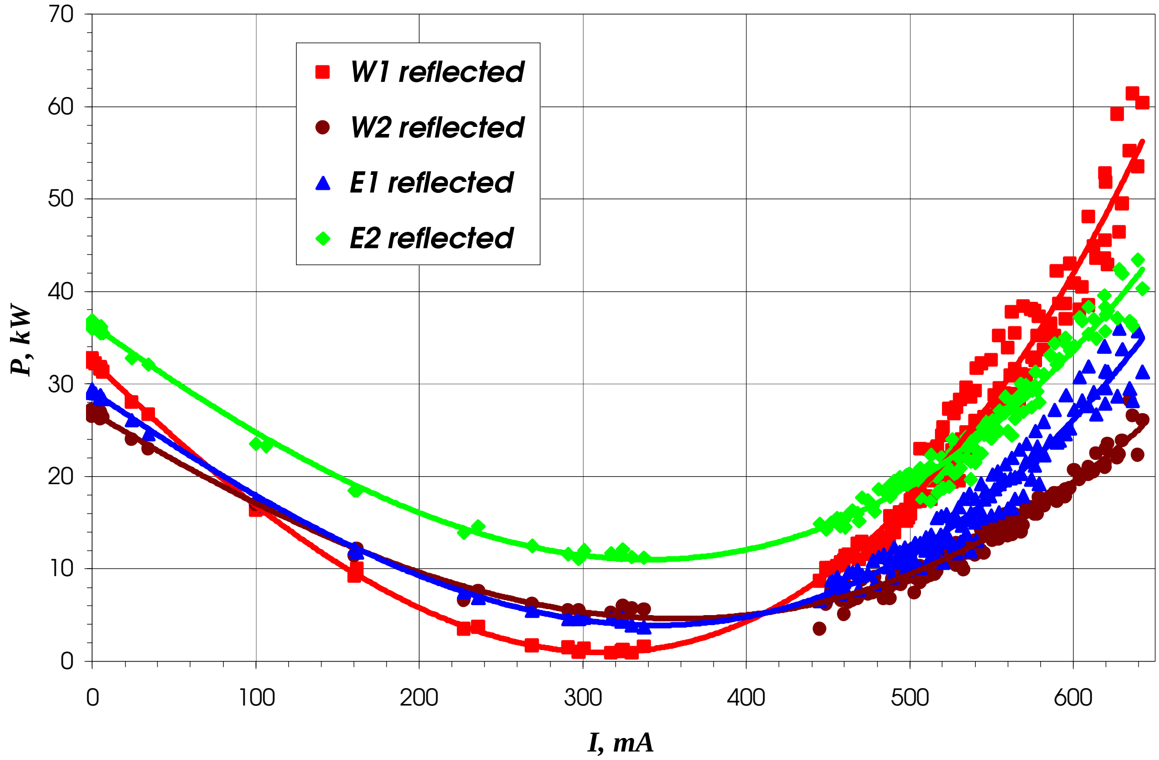

Figure 1. RF power reflected from CESR cavities vs. total beam current (minimal reflection power is not zero because the cavities are detuned from the resonance).

THEORY OF AN IDEAL TRANSFORMER

It is easy to show how the impedance transformer works using an ideal scheme (a coaxial line stub transformer is very close to the ideal scheme). The diagram of an ideal transformer with three capacitive stubs is shown in Figure 2. The transformer should match the load with normalized admittance $\boldsymbol{Y}_{\mathrm{L}}$ by appropriate stub admittances $\boldsymbol{Y}_1 = j\boldsymbol{b}_1$, $\boldsymbol{Y}_2 = j\boldsymbol{b}_2$, and $\boldsymbol{Y}_3 = j\boldsymbol{b}_3$. In fact, we need only two stubs for solving the problem. Indeed, if $\boldsymbol{Y}_{\mathrm{L}} = \boldsymbol{g}_{\mathrm{L}} + j\boldsymbol{b}_{\mathrm{L}}$ is the load admittance in the plane of the stub #1, we get matched condition ($\boldsymbol{Y} = 1$ i.e. $\boldsymbol{g} = 1$, $\boldsymbol{b} = 0$) at

$$\boldsymbol{b}_1 = \boldsymbol{g}_L \cdot \sqrt{\frac{1}{\boldsymbol{g}_L} - 1} - \boldsymbol{b}_L\,,$$

$$\boldsymbol{b}_2 = \sqrt{\frac{1}{\boldsymbol{g}_L} - 1}\,.$$

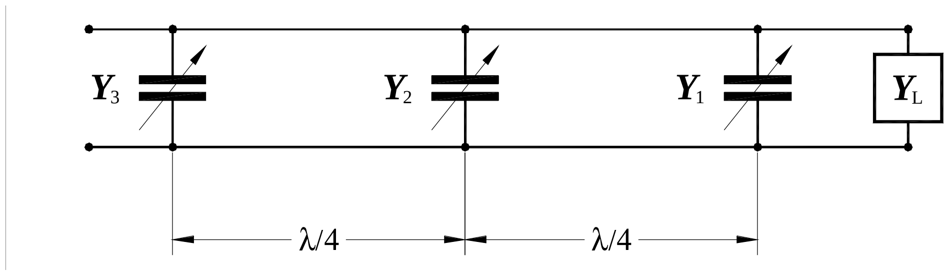

Figure 2. Diagram of an ideal 3-stub impedance transformer.

This is illustrated by a Smith chart in Figure 3. The point **1** on the chart corresponds to the load admittance $\boldsymbol{Y}_\mathrm{L} = \boldsymbol{g}_\mathrm{L} + j\boldsymbol{b}_\mathrm{L}$ (in the plane of the stub #1); after adding the stub admittance $\boldsymbol{Y}_1 = j\boldsymbol{b}_1$ we come to the point **2**. The resulting admittance is transformed to the point **3** (in the plane of the stub #2) after a regular line of a $\lambda/4$ length. And finally we come to the matched point **4** adding the stub admittance $\boldsymbol{Y}_2 = j\boldsymbol{b}_2$. The stub #3 is not used in the matching procedure ($\boldsymbol{Y}_3 = j\boldsymbol{b}_3 = 0$).

It is obvious that we cannot get the matched condition if $\boldsymbol{g}_\mathrm{L} > 1$. However, after a $\lambda/4$ line (in the plane of the stub #2) the load admittance has a real part $\boldsymbol{g}_\mathrm{L} < 1$ and in this case we should use stubs #2 and #3 instead of stubs #1 and #2 for getting the matched condition ($\boldsymbol{Y}_1 = j\boldsymbol{b}_1 = 0$ in this case). Additional restrictions appear due to practical limitations of stub admittance and for cases when the distance between stubs differs from $\lambda/4$.

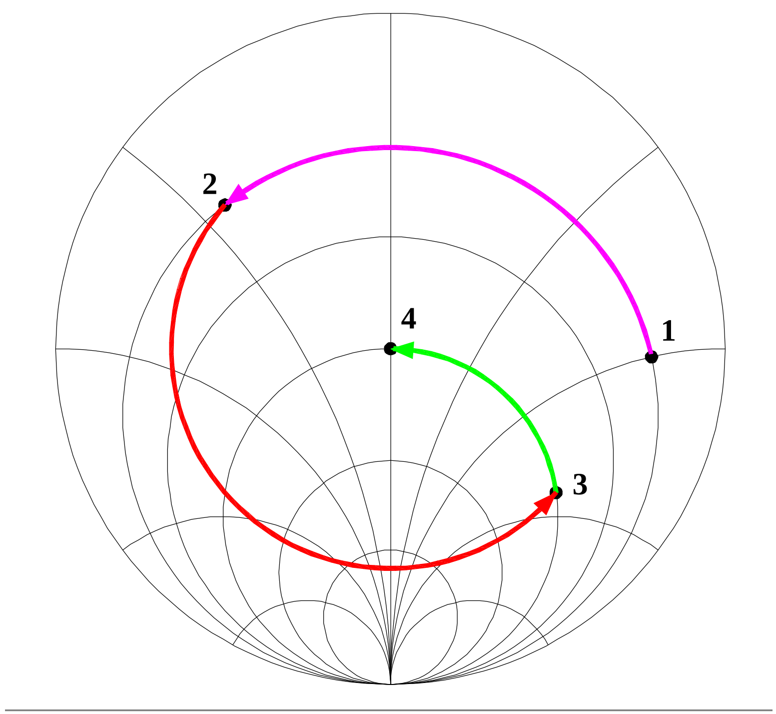

Figure 3. Matching an arbitrary load with a 3-stub impedance transformer.

REAL TRANSFORMER. CALCULATIONS AND MEASUREMENTS

RF cavities in CESR are connected to the high power klystrons by W1800 waveguides having the cross-section of $18'' \times 9''$. It was decided to make three-post waveguide impedance transformers having the scheme similar to the ideal one described above. The posts are inserting into the waveguide in the middle of its large wall where the electric field is a maximum. Waveguide impedance transformers of that type were designed and used earlier at DESY [1], [2] up to a CW power of 100 kW. We borrowed a transformer from DESY, we did its analysis [3] and successfully tested it up to 200 kW. The analysis of the design allowed expecting the reliable operation of the transformer even at higher power. Therefore we decided to use the DESY design with slight modifications. In particular, the post diameter was slightly increased for better behavior at high power levels.

We did a computer analysis of the transformer. First, we calculated scattering coefficients of a piece of the W1800 waveguide with a post in the middle of it, for different length values x of the post. The dimensions of the post are shown in Figure 4. CST Microwave Studio™ computer code [4] (a computer code developed by the same programmer team as MAFIA but providing much better accuracy for microwave applications) was used for the calculations.

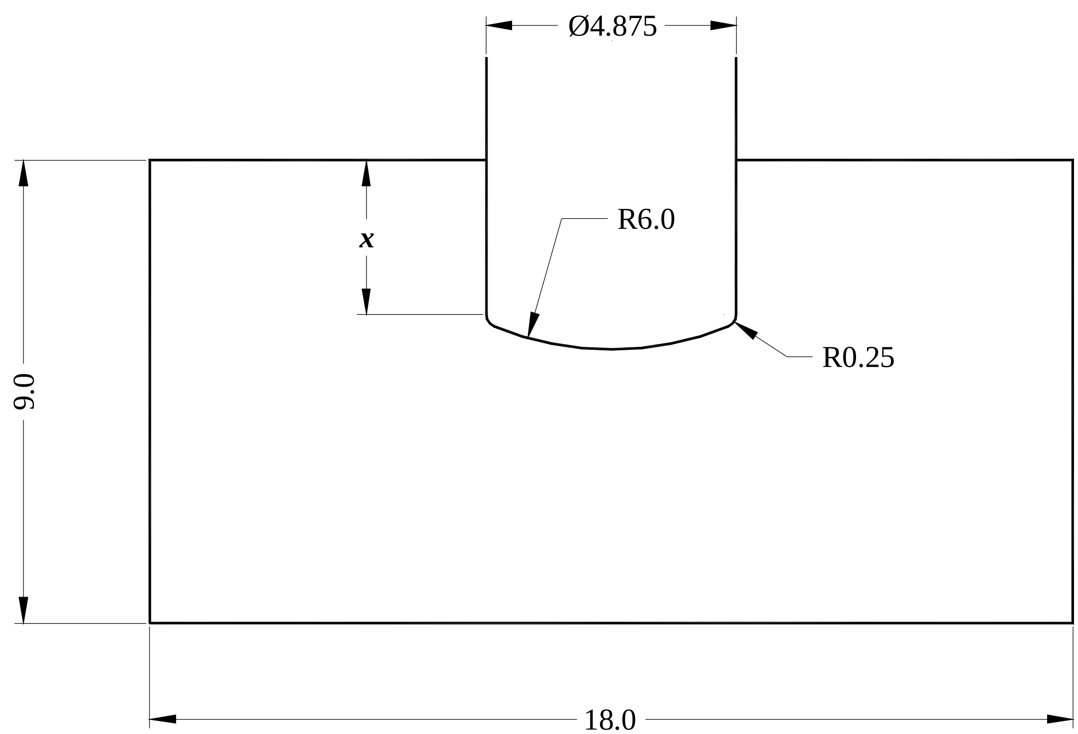

Figure 4. Cross-section of the waveguide with a post inside (dimensions in inches).

Figure 5 shows the magnitudes of $\boldsymbol{S}_{11}$ and $\boldsymbol{S}_{21}$ parameters calculated by CST Microwave Studio. In the same plot the measured values obtained for a real post in the waveguide are also shown. One can see quite a good agreement between calculated and measured numbers.

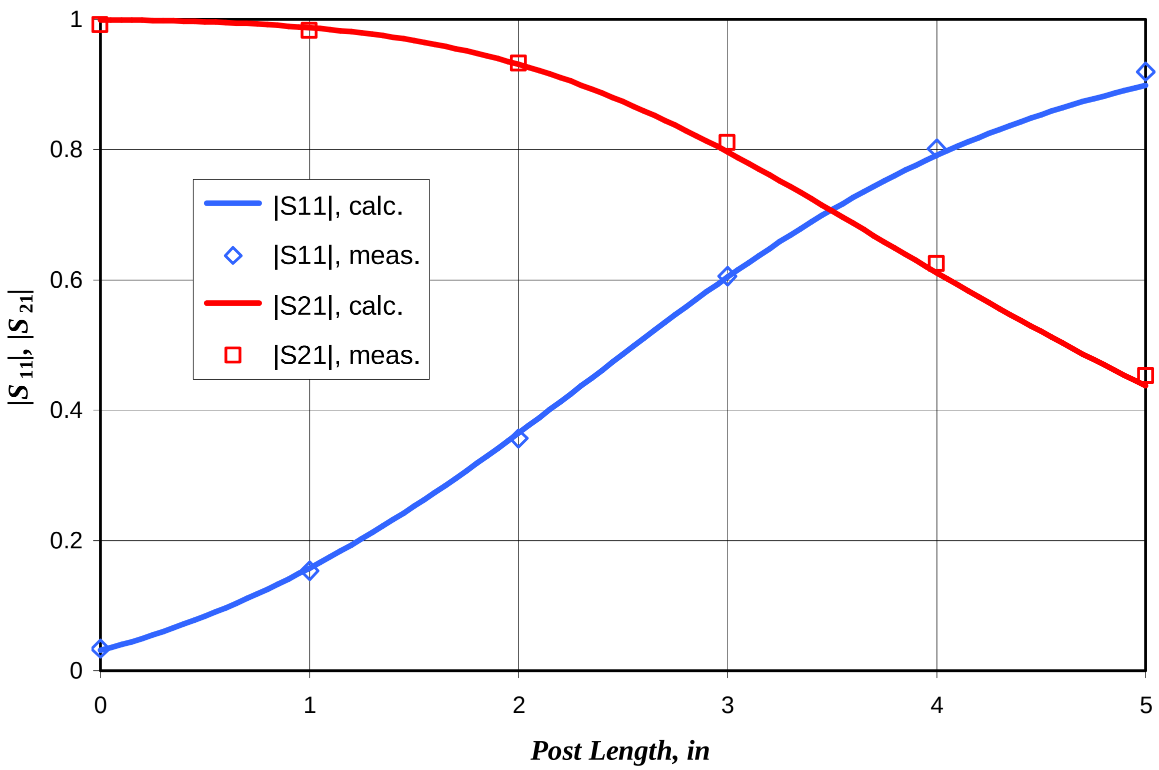

Figure 5. Calculated and measured scattering coefficients of a post inserted into the waveguide, as shown in Figure 4.

Field disturbance produced by a post in the waveguide can be described as an equivalent admittance connected to a transmission line as shown in Figure 2. This admittance is calculated by

$$\boldsymbol{Yp} = \frac{2 \cdot |\boldsymbol{S}_{11}|}{\sqrt{1 - |\boldsymbol{S}_{11}|^2}}$$

or by

$$\boldsymbol{Yp} = \frac{2 \cdot \sqrt{1 - |\boldsymbol{S}_{21}|^2}}{|\boldsymbol{S}_{21}|}$$

The chart of this admittance is presented in Figure 6 as a function of the post length.

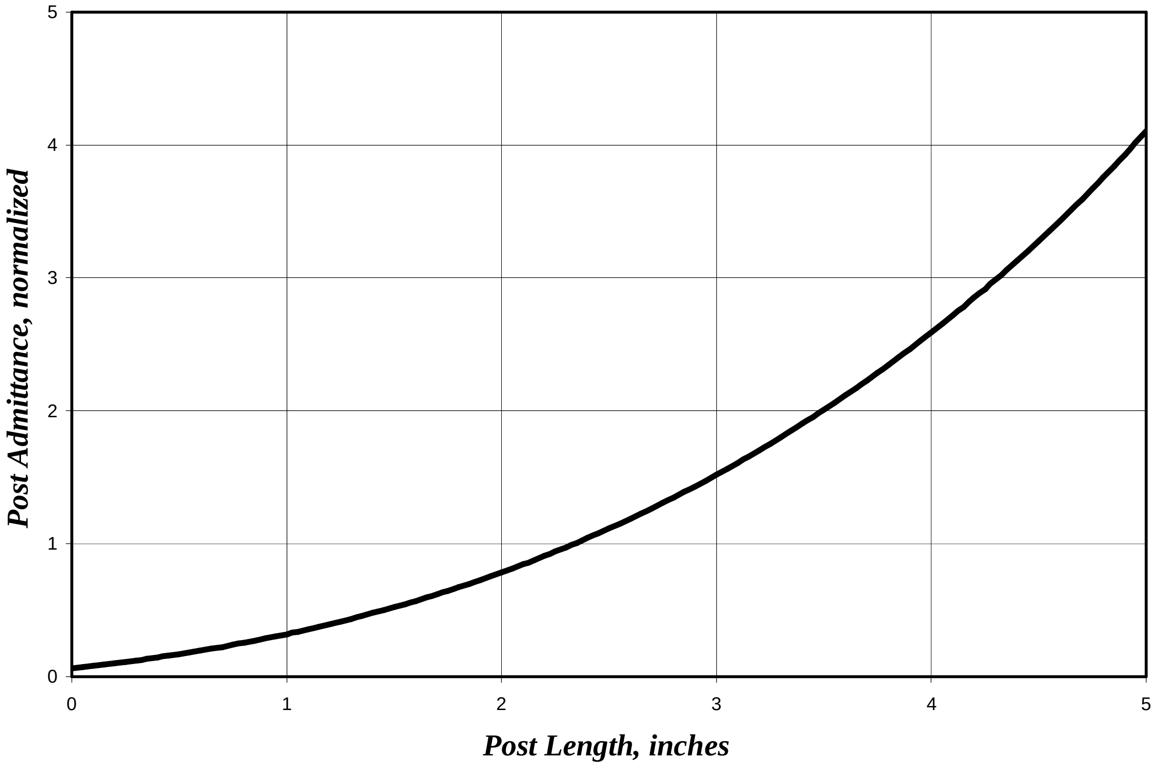

Figure 6. Calculated admittance of the post in the waveguide.

Field disturbance produced by a post causes also slowing down the wave propagation in the waveguide. Figure 7 displays the additional phase shift $\Delta\varphi$ due to this effect:

$$\Delta\varphi = -\arg(\boldsymbol{S}_{21}) - \varphi_0 ,$$

$$\varphi_0 = \frac{\omega L}{v_P} ,$$

where v_p is the phase velocity in the unperturbed waveguide, L is the physical length of the waveguide piece with the post inside, for which $\boldsymbol{S}_{21}$ coefficient was calculated, φ_0 is the phase shift of the unperturbed waveguide of the length L.

After calculation of scattering coefficients for the variety of waveguide pieces with a post of different length inside them, we analyzed the properties of the 3-post transformer using a computer model shown in the Figure 8. Each member in the network was described by a transmission matrix [$\boldsymbol{T}$]. Transmission matrix [$\boldsymbol{T}$] and scattering matrix [$\boldsymbol{S}$] are related by the following expressions:

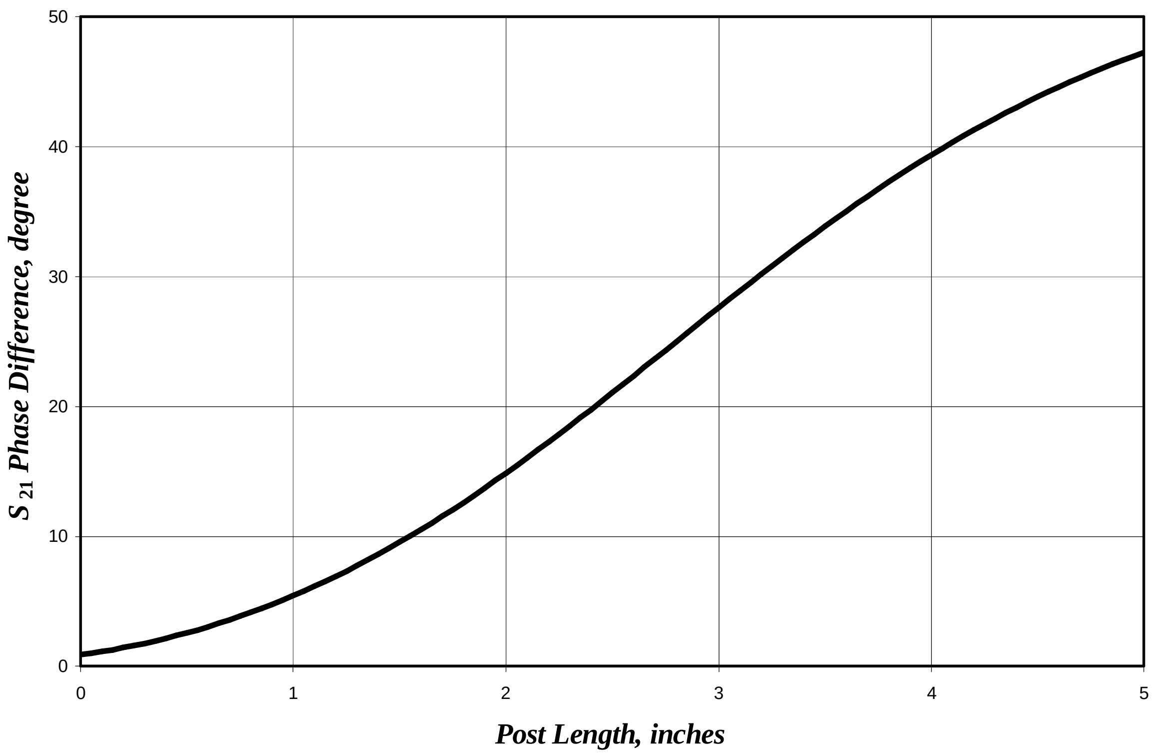

Figure 7. Additional phase shift due to the post in the waveguide.

$$[\boldsymbol{T}] = \begin{bmatrix} \boldsymbol{T}_{11} & \boldsymbol{T}_{12} \\ \boldsymbol{T}_{21} & \boldsymbol{T}_{22} \end{bmatrix} = \begin{bmatrix} \dfrac{1}{\boldsymbol{S}_{12}} & -\dfrac{\boldsymbol{S}_{22}}{\boldsymbol{S}_{21}} \\ \dfrac{\boldsymbol{S}_{11}}{\boldsymbol{S}_{21}} & \boldsymbol{S}_{12} - \boldsymbol{S}_{11}\dfrac{\boldsymbol{S}_{22}}{\boldsymbol{S}_{21}} \end{bmatrix},$$

$$[\boldsymbol{S}] = \begin{bmatrix} \boldsymbol{S}_{11} & \boldsymbol{S}_{12} \\ \boldsymbol{S}_{21} & \boldsymbol{S}_{22} \end{bmatrix} = \begin{bmatrix} \dfrac{\boldsymbol{T}_{21}}{\boldsymbol{T}_{11}} & \dfrac{1}{\boldsymbol{T}_{11}} \\ \dfrac{1}{\boldsymbol{T}_{11}} & -\dfrac{\boldsymbol{T}_{12}}{\boldsymbol{T}_{11}} \end{bmatrix}$$

Using scattering coefficients $\boldsymbol{S}_{11}$ and $\boldsymbol{S}_{21}$ from the CST Microwave Studio calculations for different post length x and knowing that $\boldsymbol{S}_{11} = \boldsymbol{S}_{22}$ and $\boldsymbol{S}_{21} = \boldsymbol{S}_{12}$, we construct the scattering matrix of a stub section [$\boldsymbol{Sp}(x)$] and hence [$\boldsymbol{Tp}(x)$].

A regular waveguide section between posts is described by the matrix

$$[\boldsymbol{Ts}] = \begin{bmatrix} e^{i\beta l} & 0 \\ 0 & e^{-i\beta l} \end{bmatrix},$$

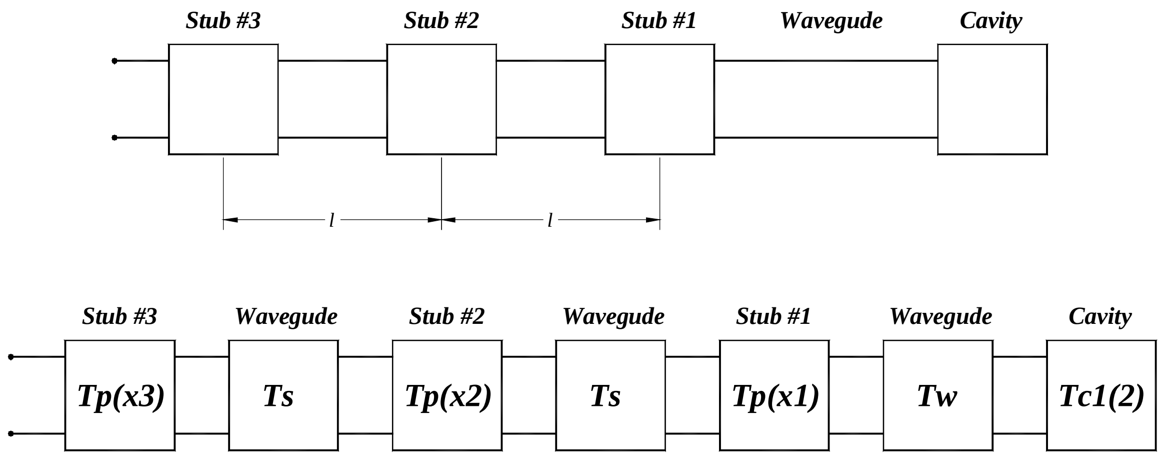

Figure 8. Scheme of cavity impedance transformation with a 3-stub waveguide transformer and a cascade connection of scheme members for computation purposes

where $\beta = 2\pi/\Lambda = \omega/v_p$ (Λ is the wave length in the waveguide, v_p is the phase velocity) is the phase constant of the waveguide, l is the distance between adjacent posts (see Fig. 8).

Similarly, the transmission matrix of the waveguide piece between the first post and the cavity is

$$[\boldsymbol{Tw}] = \begin{bmatrix} e^{i\varphi_w} & 0 \\ 0 & e^{-i\varphi_w} \end{bmatrix},$$

where φ_w is the electrical length i. e. the phase shift of that waveguide piece.

The cavity being the load connecting to the end of the waveguide is described by one of the matrixes:

$$[\boldsymbol{Tc}1] = \begin{bmatrix} \frac{1+\boldsymbol{Zc}}{2} & \frac{1-\boldsymbol{Zc}}{2} \\ \frac{\boldsymbol{Zc}-1}{2} & \frac{3-\boldsymbol{Zc}}{2} \end{bmatrix}$$

(if the cavity is represented by a normalized impedance ***Zc***) or

$$[\boldsymbol{Tc}2]=\begin{bmatrix}\frac{1+\boldsymbol{Yc}}{2} & \frac{1-\boldsymbol{Yc}}{2}\\ \frac{\boldsymbol{Yc}-1}{2} & \frac{3-\boldsymbol{Yc}}{2}\end{bmatrix}$$

(if the cavity is represented by a normalized admittance $\boldsymbol{Yc}$).

The transmission matrix of the system transformer–waveguide–cavity is obtained as a product of all matrixes:

$$[\boldsymbol{T}]=[\boldsymbol{Tp}(x3)]\cdot[\boldsymbol{Ts}]\cdot[\boldsymbol{Tp}(x2)]\cdot[\boldsymbol{Ts}]\cdot[\boldsymbol{Tp}(x1)]\cdot[\boldsymbol{Tw}]\cdot[\boldsymbol{Tc}1]$$

or

$$[\boldsymbol{T}]=[\boldsymbol{Tp}(x3)]\cdot[\boldsymbol{Ts}]\cdot[\boldsymbol{Tp}(x2)]\cdot[\boldsymbol{Ts}]\cdot[\boldsymbol{Tp}(x1)]\cdot[\boldsymbol{Tw}]\cdot[\boldsymbol{Tc}2]$$

Finally, we calculate the scattering matrix [$\boldsymbol{S}$] and look at its $\boldsymbol{S}_{11}$ term. We are interested in its magnitude

$$|\boldsymbol{S}_{11}|=\left|\frac{\boldsymbol{T}_{21}}{\boldsymbol{T}_{11}}\right|$$

In our case, we need to match the load (i. e. cavity). That means we have to find post lengths at those reflection vanishes, i. e. $|\boldsymbol{S}_{11}| = 0$.

Another parameter of interest is the phase shift, which is calculated from the phase of $\boldsymbol{S}_{21}$ term:

$$\arg(\boldsymbol{S}_{21})=\arg\left(\frac{1}{\boldsymbol{T}_{11}}\right)$$

APPLICATION TO CESR

Figure 9 displays a picture of the 3-stub waveguide transformer that was designed for CESR RF system. The distance between posts l = 9.75" is a little bigger than a quarter of the wavelength in the waveguide ($\Lambda/4$ = 7.82") due to mechanical reasons. The overall length of the transformer unit is 38". The transformers were built and installed into waveguides connecting each cavity with the RF power distribution system.

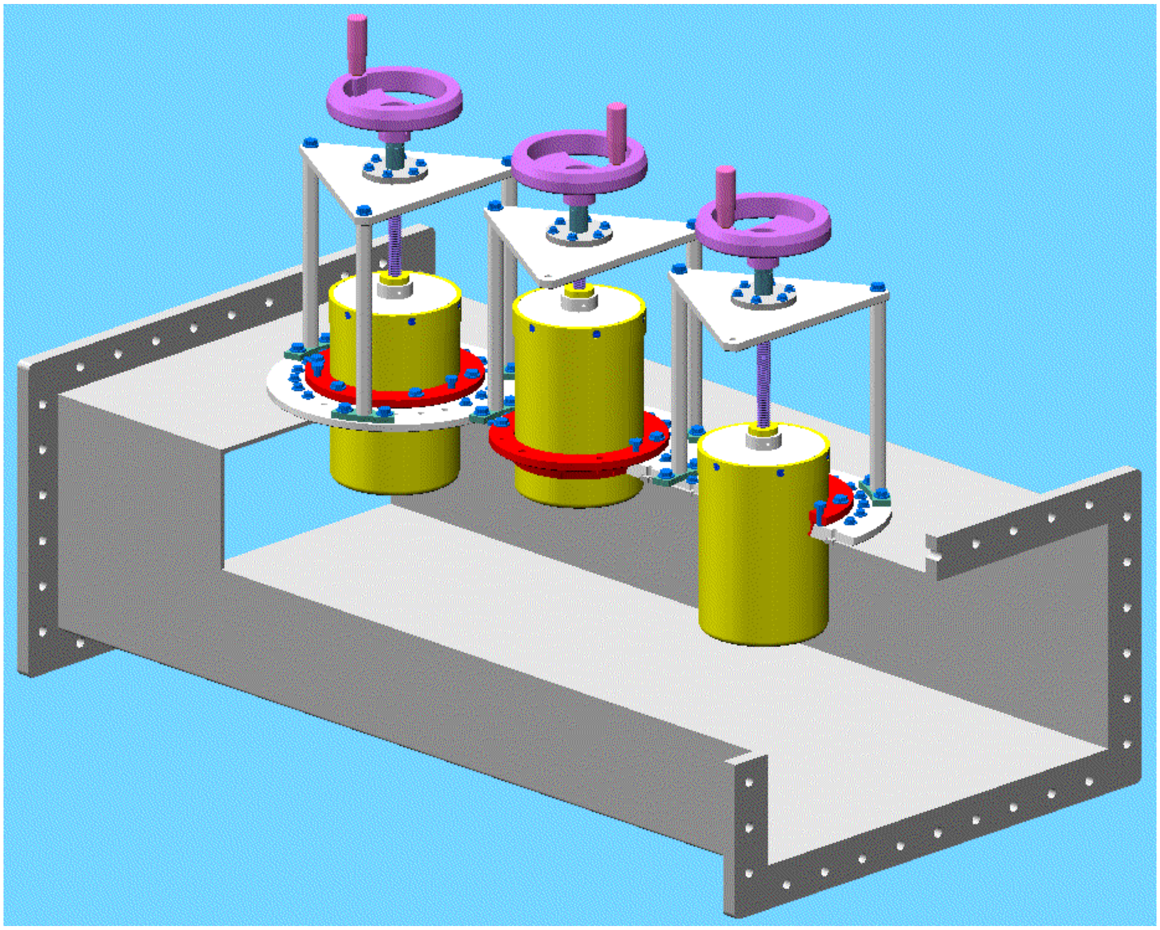

Figure 9. Design of the three-stub waveguide transformer.

Electrical lengths (phase shifts) of the waveguides from transformers to cavities were measured. They are given in the table below.

CESR Cavity	Phase shift (φ_w), degrees
E1	96.07
E2	169.05
W1	0.50
W2	175.05

Using these values, we did calculations for all four CESR cavities searching for combinations of stub positions that are required for matching different cavity impedances. As an example of the calculations, Figure 10 shows a 3d surface plot of the $|\boldsymbol{S}_{11}|$ coefficient for the E2 cavity. In that particular example, we found that for a normalized cavity impedance $\boldsymbol{Z}$ = 2 we can match the cavity i. e. obtain $|\boldsymbol{S}_{11}| = 0$ at $x1$ = 2.34", $x2$ = 1.13", and $x3$ = 1.5".

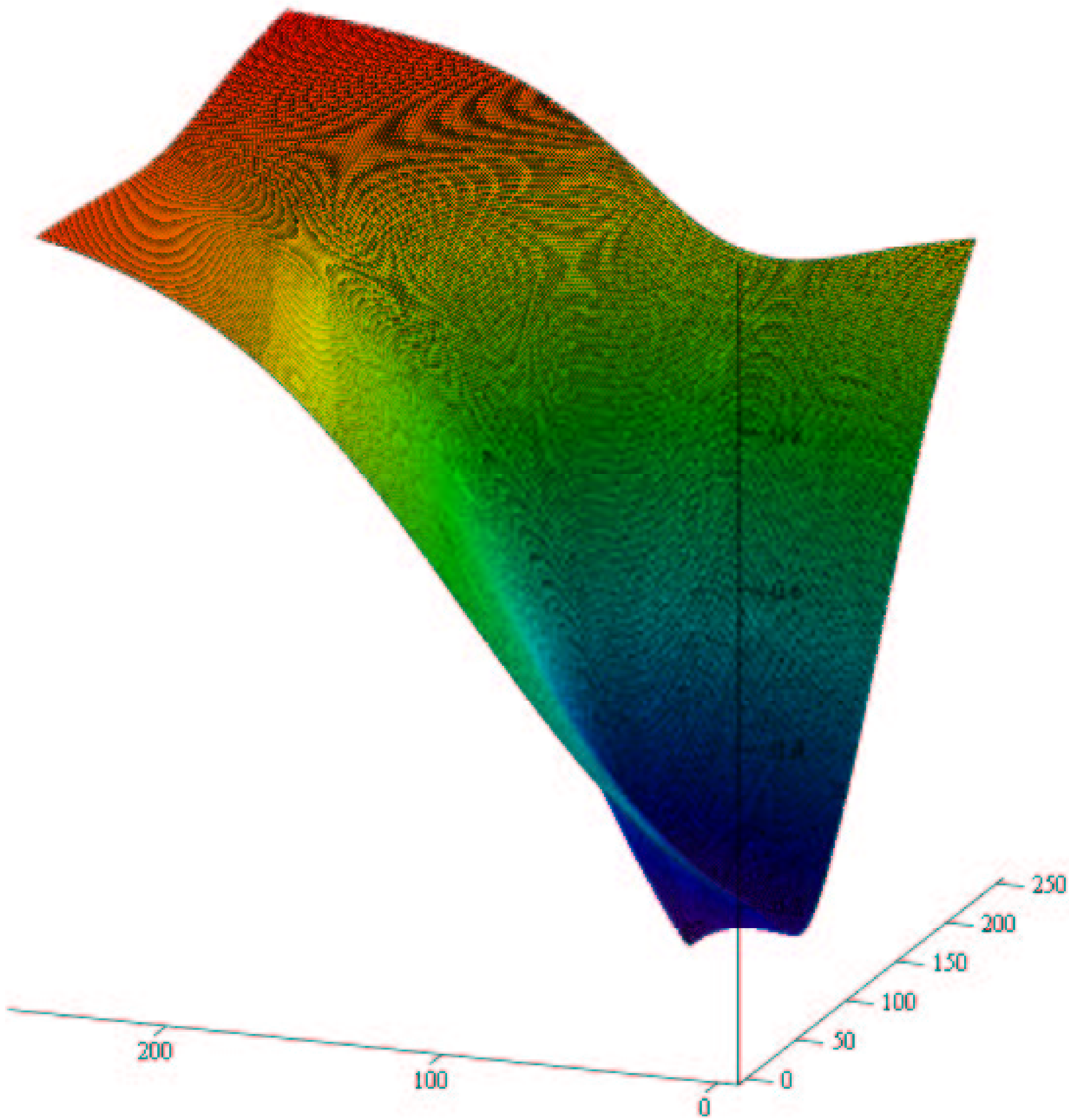

Figure 10. |$\mathbf{S}_{11}$| coefficient for E2 cavity with a normalized impedance $\mathbf{Z}$ *= 2 as a function of length of posts #1 and #2 (from 0 to 5"). The length of the post #3 is fixed at 1.5".*

The results of calculations are presented in the following batch of plots, Figure 11 to Figure 20. However, post lengths shown in the plots are not exclusive. There are always multiple possibilities to get the match.

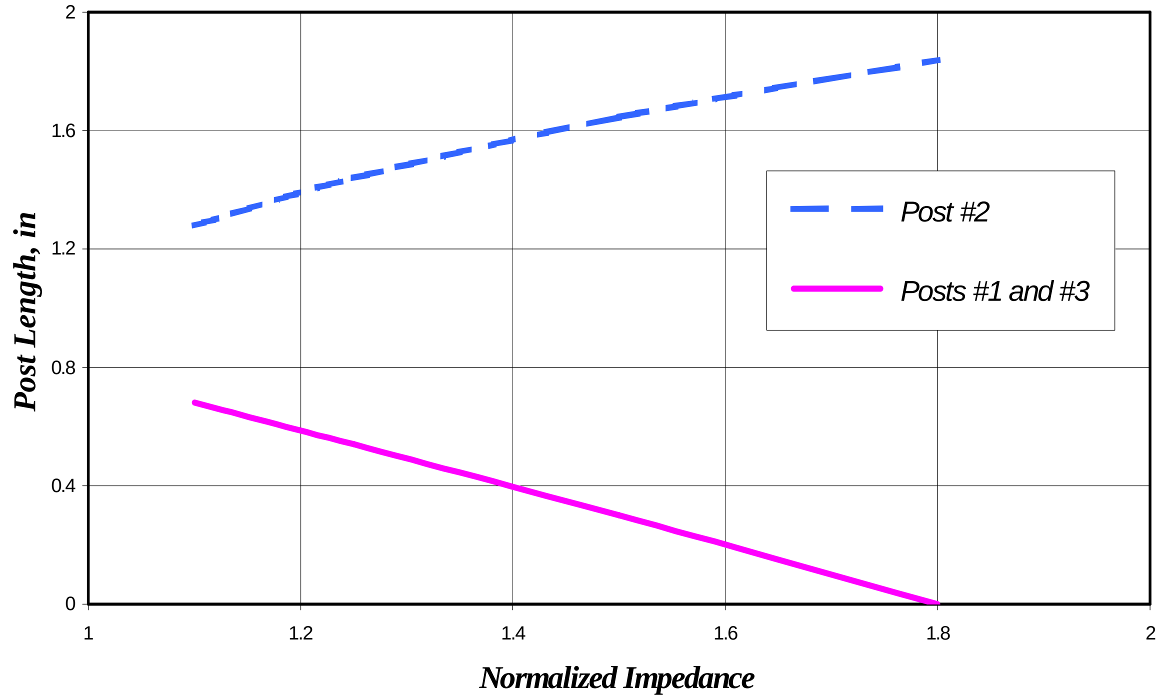

Figure 11. Post lengths for matching E1 cavity with normalized impedance in the range between 1 and 1.8.

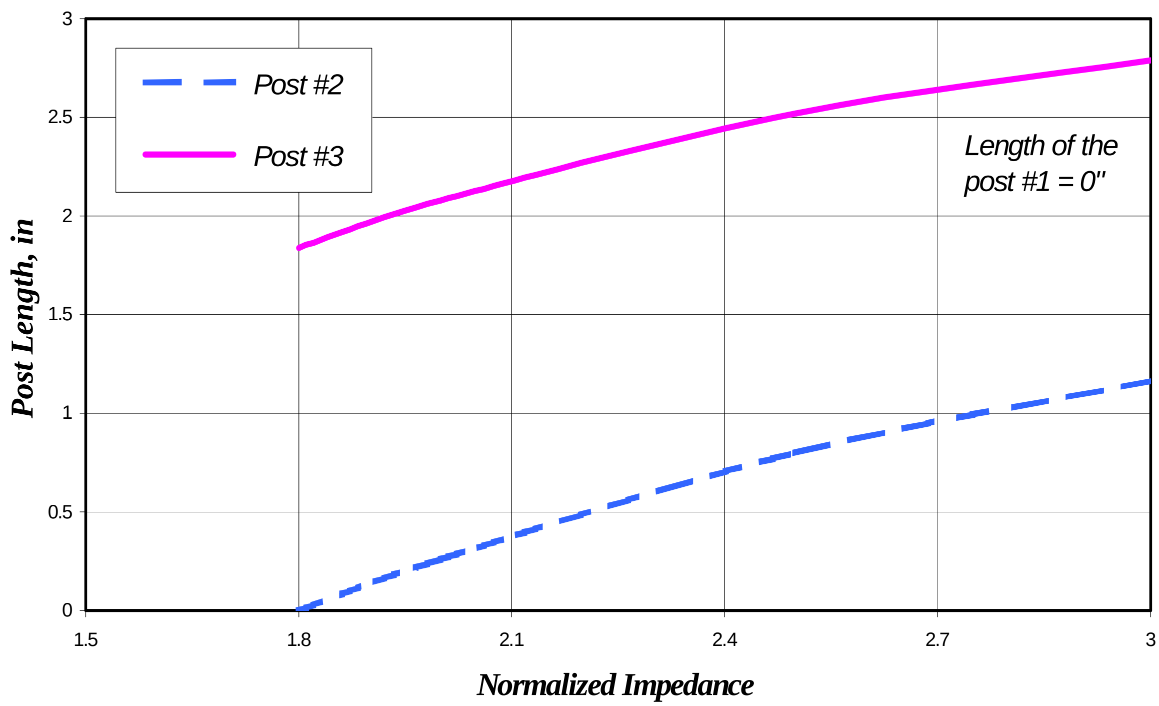

Figure 12. Post lengths for matching E1 cavity with normalized impedance greater than 1.8.

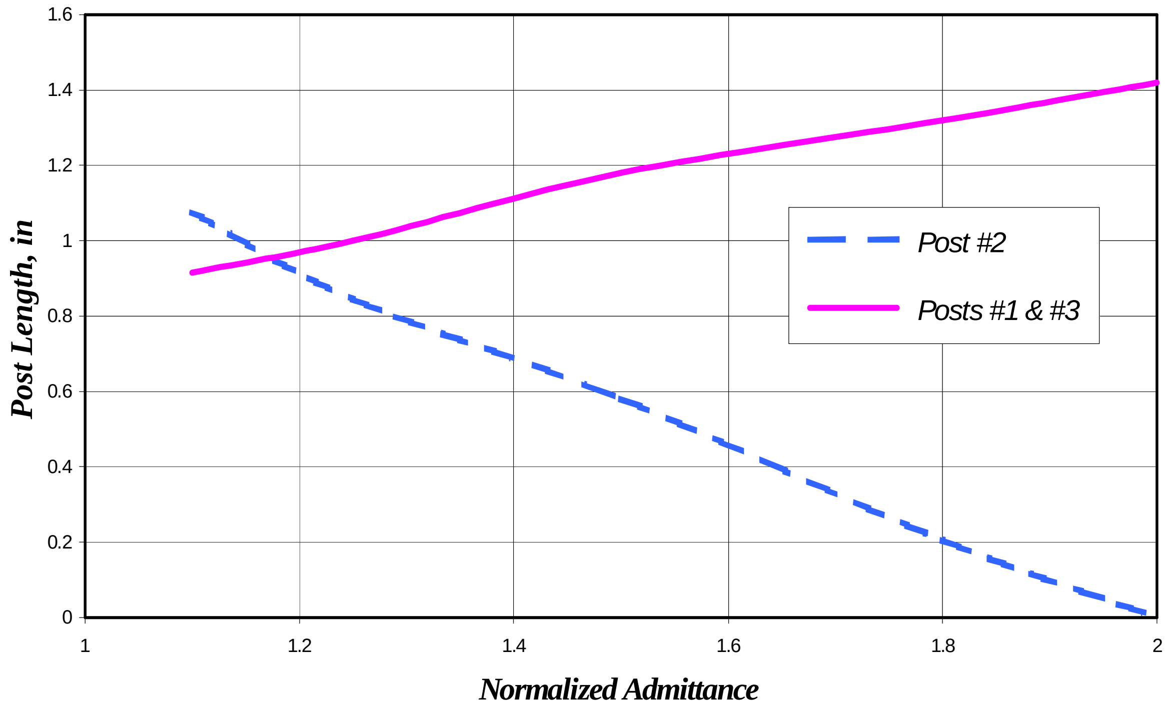

Figure 13. Post lengths for matching E1 cavity with normalized admittance greater than 1 (normalized impedance smaller than 1).

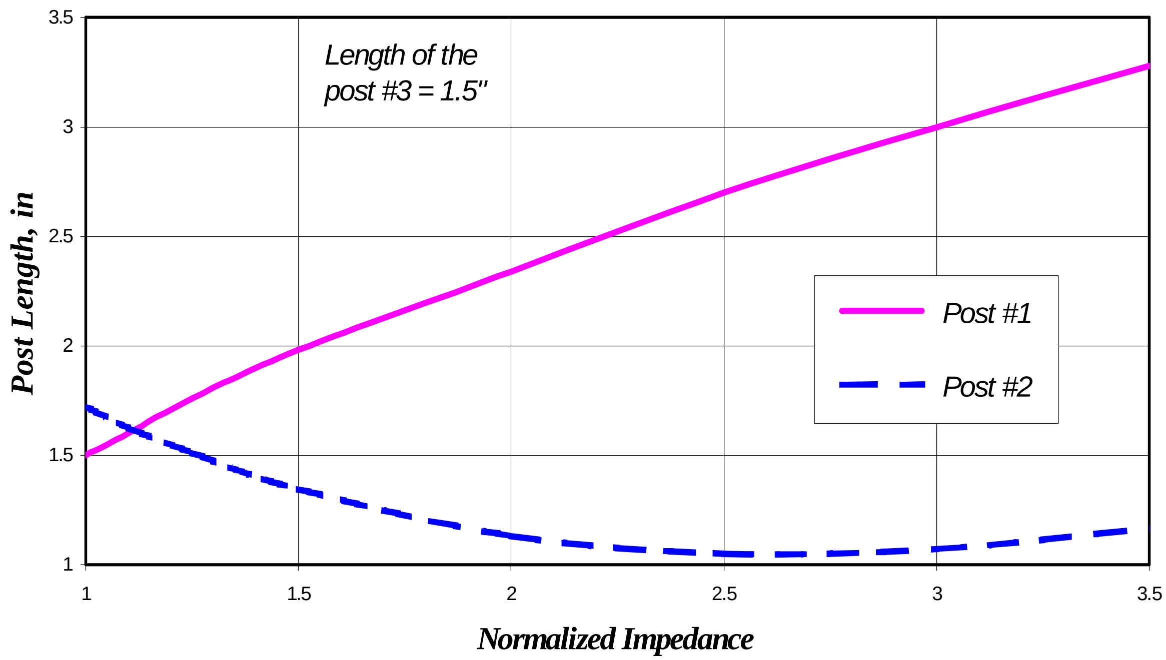

Figure 14. Post lengths for matching E2 cavity with normalized impedance greater than 1.

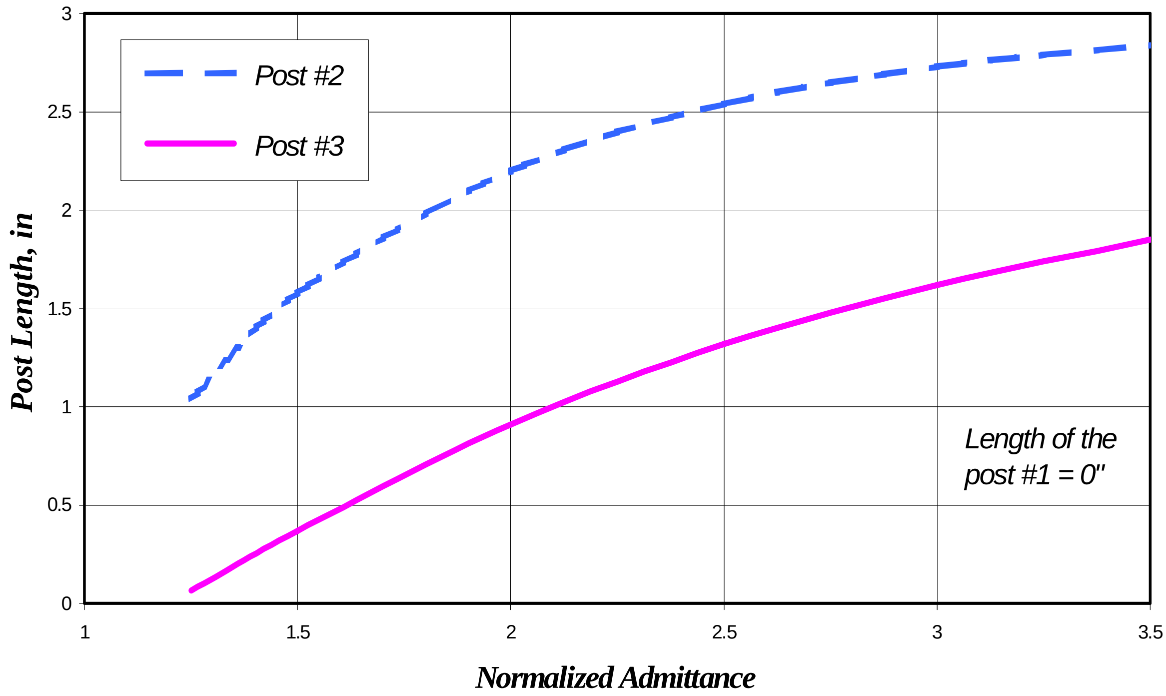

Figure 15. Post lengths for matching E2 cavity with normalized admittance greater than 1 (normalized impedance smaller than 1).

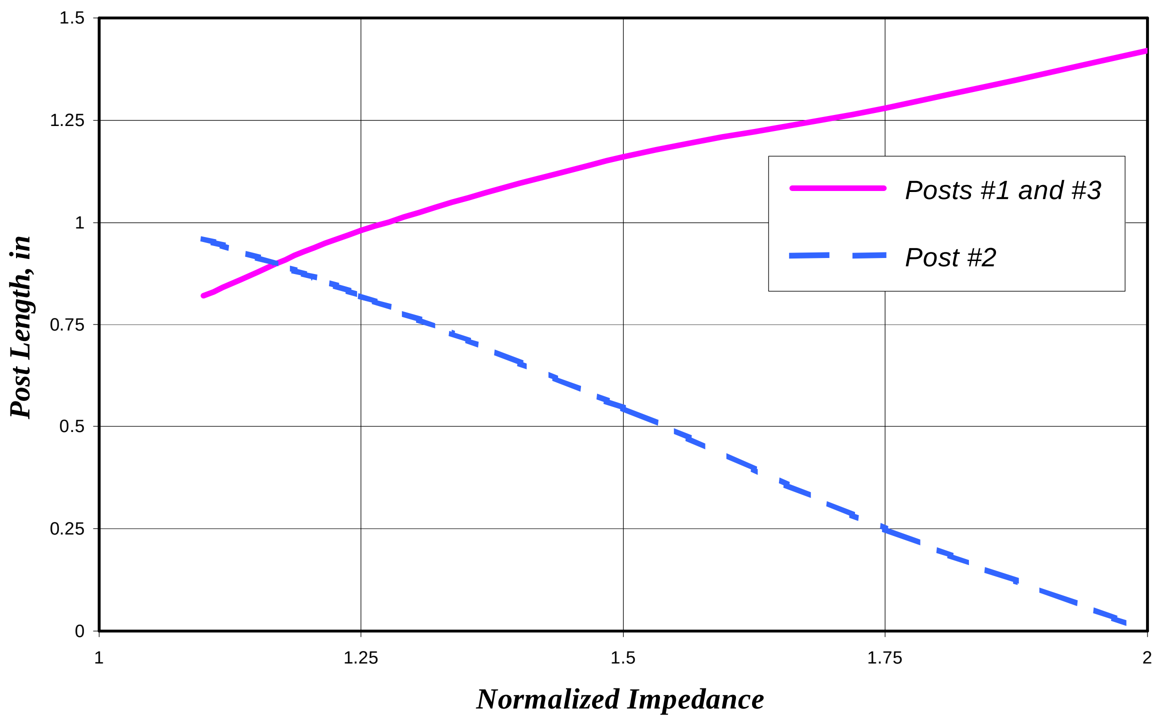

Figure 16. Post lengths for matching W1 cavity with normalized impedance greater than 1.

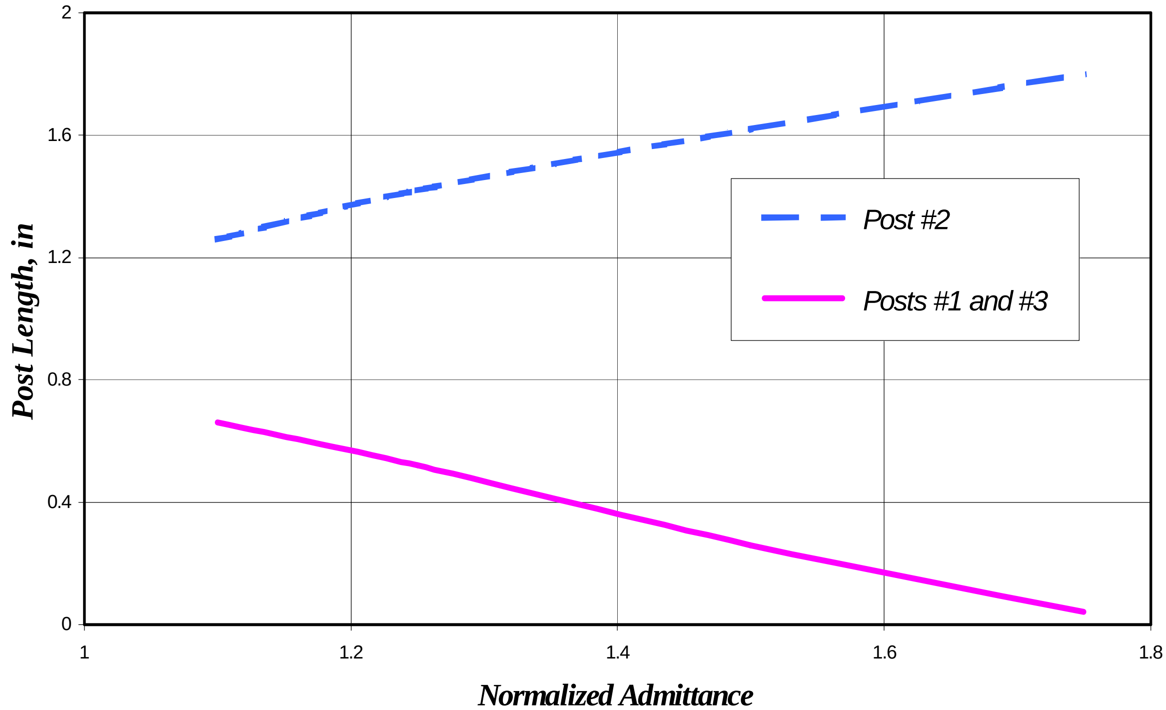

Figure 17. Post lengths for matching W1 cavity with normalized admittance in the range between 1 and 1.75.

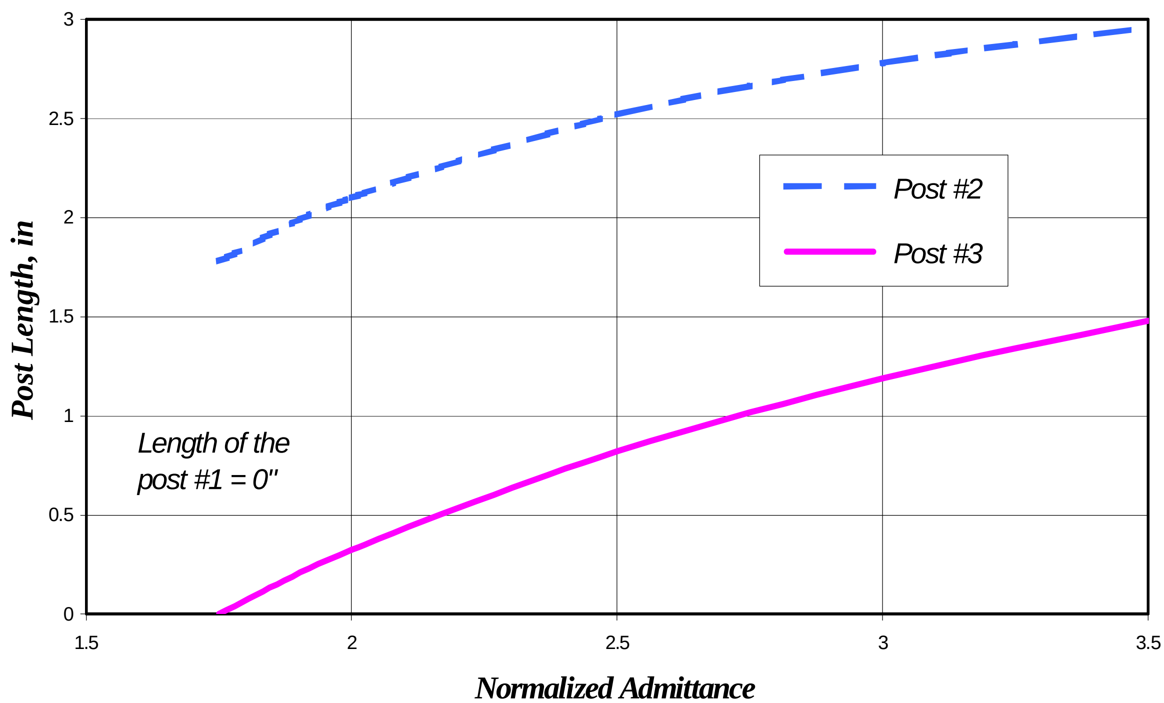

Figure 18. Post lengths for matching W1 cavity with normalized admittance greater than 1.75.

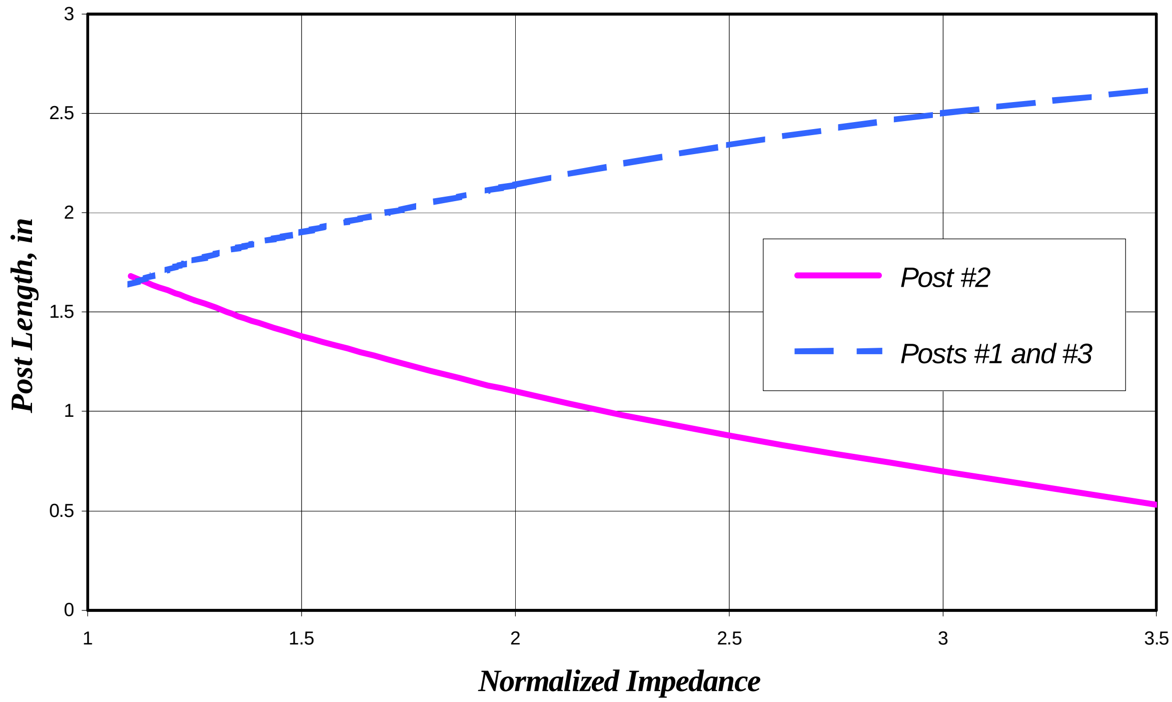

Figure 19. Post lengths for matching W2 cavity with normalized impedance greater than 1.

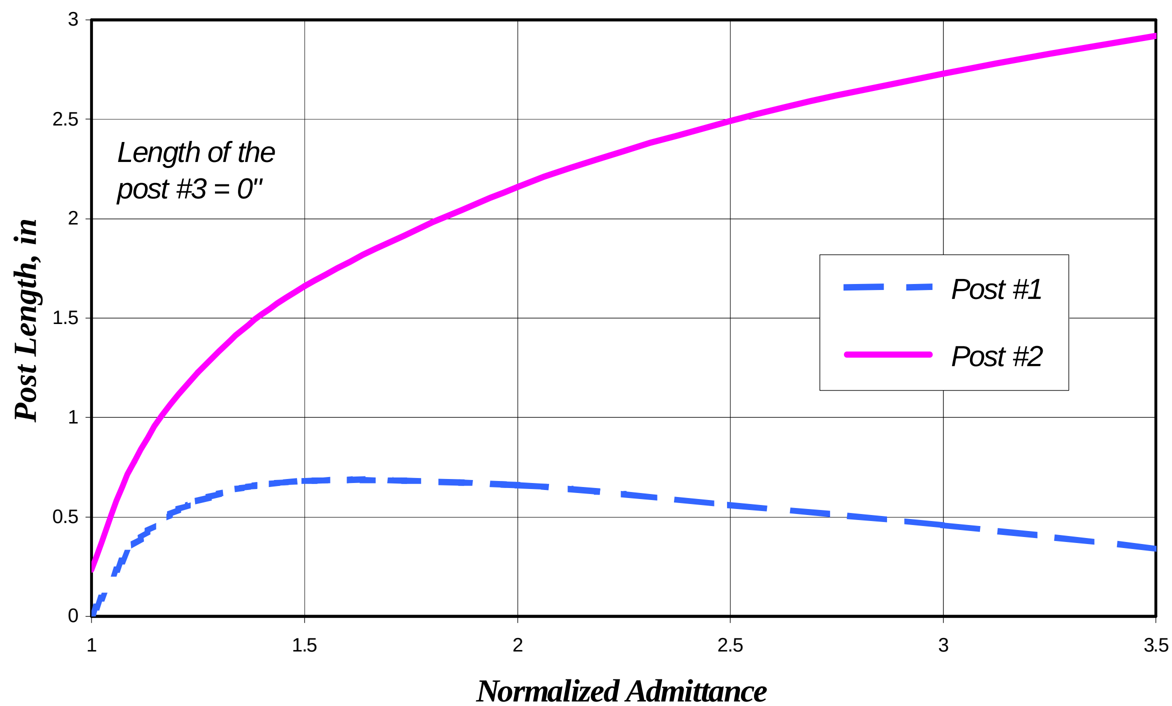

Figure 20. Post lengths for matching W2 cavity with normalized admittance greater than 1 (normalized impedance smaller than 1).

Before installation of three-stub transformers into the CESR RF system we tested one of them at high power, up to 200 kW in CW traveling wave and standing wave operation modes and up to 400 kW in traveling wave pulse mode with duty cycle = 2. As it has been predicted, there was no trace of sparking and only slight heating in the RF contact area was observed: 3°C in traveling wave mode and 6°C in standing wave mode. For reference, Figure 21 shows the magnetic field distribution on the large wall of the waveguide with two three-inch posts.

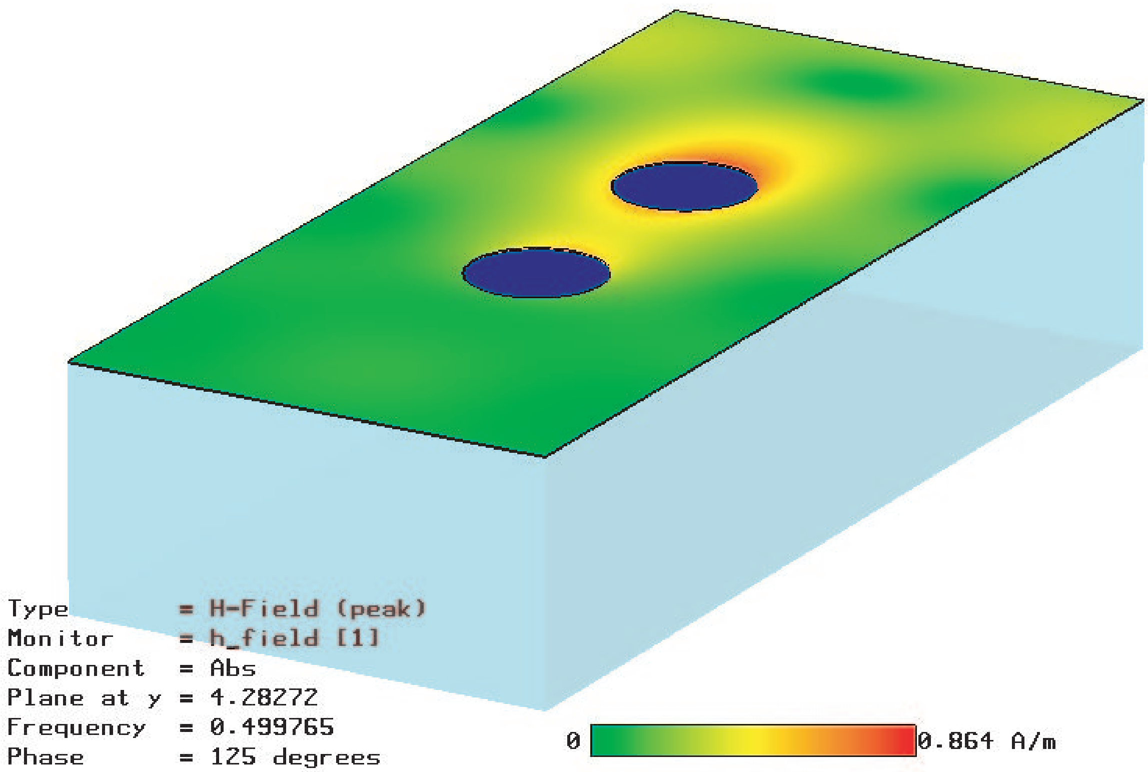

Figure 21. Distribution of magnetic field on the large wall of the waveguide with posts of 3" long each.

After installation, the impedance transformers were used to correct too strong coupling of E1 cavity (impedance transformation ratio 2) and to equalize impedances of west cavities (impedance transformation ratio 1.2).

CONCLUSION

Three-stub high power waveguide impedance transformer based on DESY concept was designed for CESR RF system. Five transformers were built. Four of them were mounted into waveguides between CESR cavities and klystrons and one transformer was installed in the high power test facility. Transformers were successfully used for equalizing impedances of CESR cavities what improved operation of CESR RF system. RF system equipped with high power waveguide impedance transformers has been in operation since September 2001. The maximum RF power in a transformer during the operation was 200 kW.

The presence of impedance transformers improves flexibility of RF system. That will be very useful in future in CESR-c project when the beam loading will be significantly lower.

REFERENCES

[1] B. Dwersteg, Q. Yufang. High RF Power Waveguide Transformer. Report DESY-M-89-08, 1989.

[2] B. Dwersteg. SC-Cavity Operation via WG-Transformer. In: Proceedings of the 4th Workshop on RF Superconductivity, Vol. II, pp. 593–604. KEK Report 89-21, 1989.

[3] C. Chen. Matrix Model of the Waveguide Transformer. Cornell LNS Report SRF 010219-02, 2001.

[4] CST Microwave Studio™. CST GmbH, Darmstadt, Germany.